9th International Conference on Contact Mechanics and Wear of Rail/Wheel Systems
(CM2012), Chengdu, China, August 27-30, 2012

100-FOLD SPEED-UP OF THE NORMAL CONTACT PROBLEM AND OTHER RECENT DEVELOPMENTS IN "CONTACT"

Edwin A.H. Vollebregt[1)2)*]
1) DIAM, Delft University of Technology, The Netherlands
2) VORtech BV, Delft, the Netherlands
* e.a.h.vollebregt@tudelft.nl

ABSTRACT

In this paper we present recent and ongoing developments with respect to Kalker's CONTACT software. One notable achievement concerns the extension of the model with respect to effects of roughness, contaminants and temperature. These are included in an indirect, parameterized way, by adding an interfacial layer and by refining the friction law. With these extensions we can describe the reduced slope and the falling behaviour of measured traction curves. Other developments concern a 100-fold speed improvement for solving normal contact problems and the integration of CONTACT in the multi-body simulation software SIMPACK Rail.

1 INTRODUCTION

The railway system is a very complex one, with strong and subtle interactions between the different components of the vehicle, within the track system and in the wheel/rail interface. There are many variables that have a strong effect on cost, durability and performance of the system: bogie design and maintenance, wheel and rail profiles, metallurgy, track stiffness and alignment, etc. [1]. Because of the strong and non-linear interactions, simulation is an important tool for understanding the system behavior [11]. Simulation allows to repeat "experiments" easily, access all parameters separately and to do parametric studies and optimization as well.

In the last decades we have seen a tremendous increase in simulation capabilities for railway vehicles. Vehicle dynamic simulation (VSD) has become a well established tool for vehicle designers and track engineers for investigating problems with ride quality, derailments, excessive damage and wear. However, we are continuously challenged to extend the range of applications for which simulations can be used, and to increase the degree of realism, detail and accuracy, thereby keeping the computation time to a minimum.

A special role in this is played by the interaction phenomena between wheel and rail. On the one hand these con-

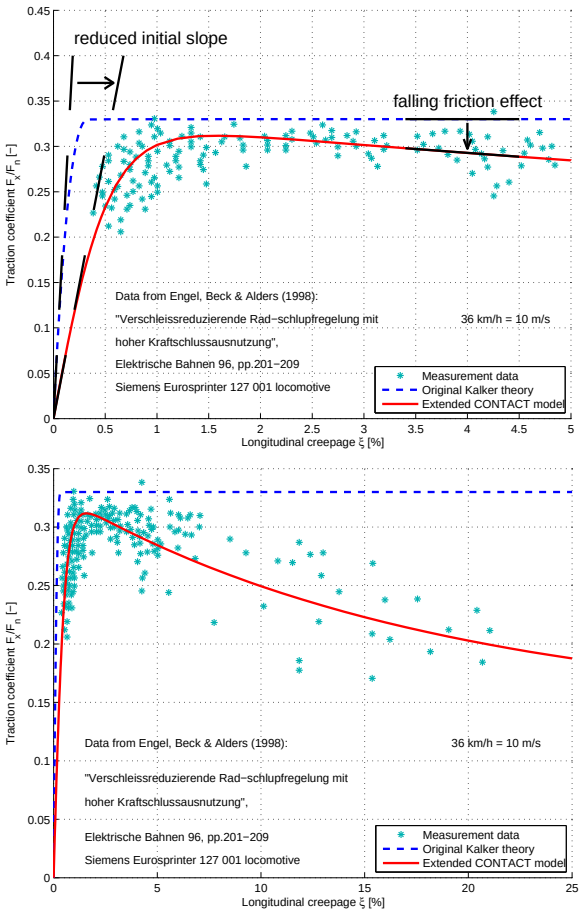

Figure 1: *Measured and computed creep forces for the Siemens locomotive Eurosprinter 127001 for pure longitudinal creepage.*

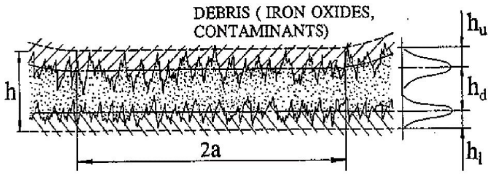

Figure 2: *Schematic illustration of an interface layer of contaminants and debris between wheel and rail by Hou et.al. [6].*

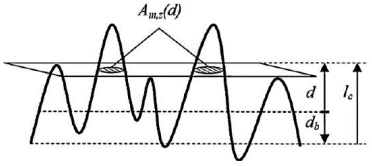

Figure 3: *Schematic illustration of surface roughness and real area of contact by Tomberger et.al. [13].*

stitute the forces between the vehicle and the track, and thus govern the dynamic behavior of the system components. Therefore all vehicle system dynamics simulation packages contain a wheel/rail contact force model in one or another form. On the other hand, the stresses in the interface are important as well. Such high and variable stresses occur, with consequent damage and wear, that these contribute significantly to the overall system cost.

Different types of contact models exist and are used for different purposes. In general three different classes can be discerned:

1. Fast and approximate approaches, such as FASTSIM2 [19], Polach's method [10] and table-lookup schemes. These are used to get the forces that are needed in dynamic simulations, but are not well suited for more detailed contact studies;
2. Half-space based approaches, particularly CONTACT [15], which are physics-based theories for specific geometries and materials;
3. Finite element approaches that are fully generic and flexible in principle, but that take high calculation times [20].

More information is presented in [16], where CONTACT is used to assess the accuracies of various simplified rolling contact algorithms. This shows that for the contact forces in a vehicle simulation one should preferrably use a table-based approach. If one needs more flexibility, for instance with respect to non-elliptical contact patches [7] or a velocity dependent friction law [5] then FASTSIM2 is the best alternative. This yields total forces that typically differ less than 10% to the CONTACT results, except in situations with larger spin creepage, where differences larger than 20% occur 15-20% of the time.

More detailed modeling is needed for investigation of wear and RCF and for instant for transient phenomena such as squeal noise. In these cases one is less interested in the overall force than in its distribution in the contact patch. In such cases one should use a half-space based approach where possible and revert to finite element approaches otherwise. In this paper we describe recent developments with respect to the CONTACT software, that extend the range of CONTACT's applicability.

2 INITIAL SLOPE OF THE TRACTION CURVE

A comment on Kalker's rolling contact theories is that they describe well only the situation for *scrupulously clean surfaces* [8]. In many measurements of traction curves a reduced initial slope is found (Figure 1). This is generally attributed to the effects of contamination (Figure 2) and of surface roughness (Figure 3).

These effects are incorporated in CONTACT by modeling a third body layer as illustrated in Figure 4. Vertical deformation in the layer is ignored. The total elastic deformation at a point $\mathbf{x}$ is

$$\mathbf{u}_t(\mathbf{x}) = \mathbf{u}_t^{(1)}(\mathbf{x}) - \mathbf{u}_t^{(2)}(\mathbf{x}) + \mathbf{u}_t^{(3)}(\mathbf{x}), \tag{1}$$

where the deformation in the layer is described with:

$$\mathbf{u}_t^{(3)}(\mathbf{x}) = \frac{\mathbf{p}_t^{(1)}(\mathbf{x})\, h^{(3)}}{G^{(3)}}. \tag{2}$$

Here $h^{(3)}$ is the thickness of the layer and $G^{(3)}$ its shear modulus. Note that the deformation in the layer is a function of the local shear stress alone, as if the layer consists of independent springs. This can be understood directly in terms of the view of surface roughness of Figure 3. It is also consistent with the model provided by Hou et.al. in [6].

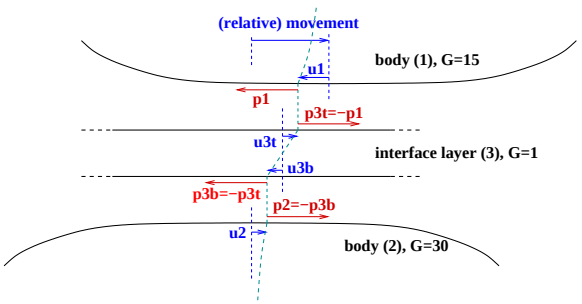

Figure 4: *Illustration of tractions* $\mathbf{p}_t^{(a)}$ *acting on bodies* $a = 1..3$ *and displacements* $\mathbf{u}_t^{(a)}$ *in the bodies as a result of (gross) relative movement.*

By increasing the thickness or reducing the shear modulus we increase the amount of deformation taken up by the layer instead of by the bulk materials. This reduces the tractions that are required and therby reduces the slope of the traction curve.

Equation (2) is the same as the tractions to displacement relation that is used in the simplified theory ($\mathbf{u}_t = L\mathbf{p}_t$). Note however that the interaction between different points is still incorporated via the elastic behavior of the bulk materials ($\mathbf{u}_t^{(1)}$ and $\mathbf{u}_t^{(2)}$ in (1)). The system of equations to be solved therefore largely remains the same. The interface layer appears to be favourable in this: it contributes to the diagonal of the system matrix and thus makes the system easier to solve.

3 VELOCITY-DEPENDENT FRICTION

A second effect that is found in measured traction curves and not incorporated in Kalker's theories is a decrease of the creep force with increasing creepage after attaining a maximum (Figure 1). This is called "falling friction", and is thought to be an important factor in the generation of squeal noise. The velocity-dependence is generally attributed to the effects of temperature and may further be due to the effects of fluids in the interface.

Velocity dependence is incorporated in CONTACT by assuming the friction coefficient μ to be dependent on the absolute local slip velocity $s_a = V \cdot \|\mathbf{s}_t(\mathbf{x})\|$. A typical friction law that is used is

$$\mu_s(s_a) = \mu_{kin} + (\mu_{stat} - \mu_{kin}) \cdot e^{-\log(2)\, s_a / s_{hlf}}. \qquad (3)$$

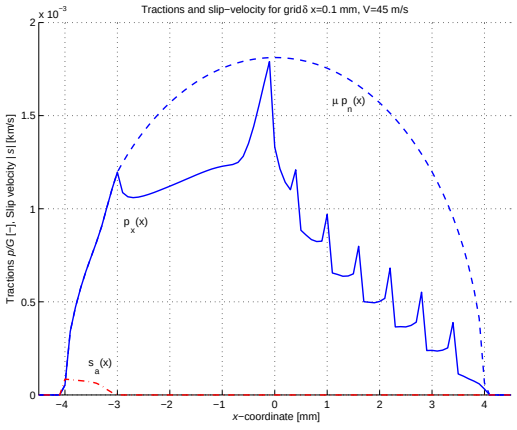

Figure 5: *Tangential traction distribution for a rolling cylinder with falling friction, illustrating instabilities in transient rolling scenarios.*

Here μ_{kin} is the asymptotic value of the friction coefficient for $s_a \to \infty$, and s_{hlf} is the slip velocity at which the contribution $\mu_{stat} - \mu_{kin}$ of the second term is halved.

The replacement of the Coulomb friction law by (3) makes the equations to be solved more complicated. This is solved via an additional iteration procedure as described in [17]. The model extension works well for steady state rolling scenarios. For large creepages the results are dominated by the friction law that is used. This can be understood easily because when full sliding occurs, the local slip $\mathbf{s}_t(\mathbf{x})$ is dominated by the creepage, which is then largely the same for all $\mathbf{x}$ in many scenarios.

The model extension comes with surprising results for transient rolling scenarios. Certain instabilities are found in all cases except when a very coarse grid discretization is used together with sufficiently large s_{hlf} (slow response of μ_s to slip velocity). These instabilities consist of a sudden collapse of the shear tractions and corresponding peak in the slip velocity. In order to maintain adhesion in part of the contact area after the collapse, the tangential tractions quickly increase at the leading edge of the contact. This gives peaks in the traction distribution, that travel from the leading edge through the contact area (Figure 5).

The peaks are analyzed in detail in [17]. They are attributed to the instantaneous reaction of the friction law

to the instantaneous local slip velocity s_a. It is interesting to see that similar complications are found when (3) is used in the FASTSIM approach [9]. A considerable difference is that instabilities are found in CONTACT only for transient simulations, whereas they occur in FASTSIM in steady state situations too. This is because in FASTSIM the tangential displacements $\mathbf{u}_t(\mathbf{x})$ and thereby the slip $\mathbf{s}_t(\mathbf{x})$ respond instantaneously to the local shear stress $\mathbf{p}_t(\mathbf{x})$. Indeed, when the falling friction law (3) in CONTACT is combined with the interface layer (2), instabilities occur in CONTACT in steady state situations too. Note that the model presented in [13] is also based on the simplified theory. Therefore we suspect that it is also troubled by artefacts and strong dependence on the grid resolution.

The instabilities that arise because of falling friction are regularized by introducing *friction memory*. The friction coefficient μ_s of (3) is interpreted as the steady state friction that arises at continuous sliding at velocity s_a. It is distinguished from the actual coefficient of friction $\mu = \mu(\mathbf{x},t)$. The relaxation of μ to μ_s is described by

$$\dot{\mu}(\mathbf{x},t) = -\frac{max(s_a(\mathbf{x},t),s_0)}{d_c}\left(\mu(\mathbf{x},t) - \mu_s(s_a(\mathbf{x},t))\right) \quad (4)$$

Here $\dot{\mu}$ is the particle-fixed time derivative, d_c is a characteristic slip distance over which the relaxation occurs, and s_0 is a minimum value for the slip velocity, that allows adaptation of μ in the adhesion area.

The concept of friction memory comes from the rate- and state-dependent friction laws that are widely used in the earthquake community [3, 12]. The physical motivation is that the actual contact takes place at the tips of asperities (cf. Figure 3), that the strength of asperity contacts increases over time due to plastic creep, and that the friction reduces by breaking some contacts and replacing them by new ones. The amount of local sliding that is needed to break the contact is of the order of the size of the asperities themselves. Therefore typical values for the memory distance d_c are in the order of micro-meters.

4 NEW RESULTS

The main result of the developments that are presented above is the capability to reproduce creep force measurements. This is illustrated in Figure 1 for measurements presented by Engel et.al. [4] which were used before by Polach for testing his approach [10].

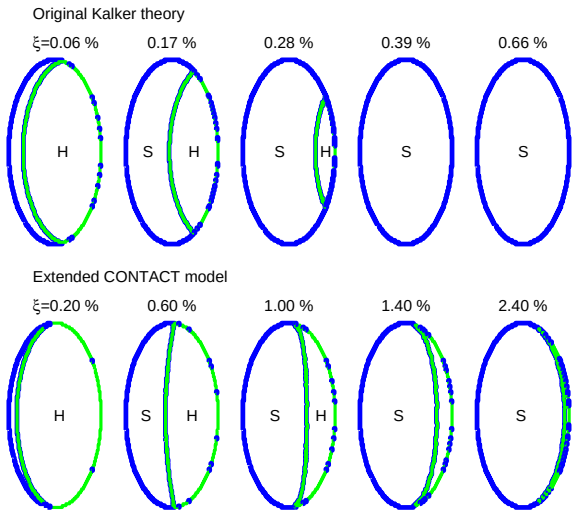

Figure 6: *Size and shape of the adhesion (H) and slip areas (S) for rolling with pure longitudinal creepage.*

The parameters used in this experiment closely resemble those used in [10]. The wheel load and radius are $F_n = 106.7\,kN$ and $625\,mm$, and the contact patch has semi-axes $a = 6.3$ and $b = 12.6\,mm$. The rolling velocity is $V = 10\,m/s$. The parameters of exponential friction law (3) are $\mu_{stat} = 0.33$, $\mu_{kin} = 0.140$, $s_{hlf} = 1.25\,m/s$. For the friction memory, the memory distance is $d_c = 0.003\,mm$ and $s_0 = 0.001\,m/s$. An interface layer is used with $G^{(3)} = 82000\,N/mm^2$ and thickness $0.125\,mm$. This reduces the initial slope of the creep force curve by a factor 3.62.

The fit of the new model with the measurements (Figure 1) is as good as that of Polach's approach. In comparison, the transition from the increasing to saturated regimes is spread out more in Polach's approach, and it also reaches a lower percentage of the maximum friction (μ_{stat}). A further difference is of course that Polach's approach is an approximation of the simplified theory, which is very fast but only works well for straight running where the spin creepage is small. The new results are obtained with the physics-based CONTACT model, which is much slower, but which is applicable to a much wider range of situations too.

The interface layer appears to have a strong effect on the size and shape of the adhesion and slip areas. This is shown in Figure 6 for different points along the traction curve (Figure 1). Note that 3.62 times smaller creepages are used for the original approach, in order to compare points with comparable total force. The slip area is smaller and grows much slower in the presence of the interface layer, and at larger creepages it becomes convex instead of staying concave. The consequence of this is not entirely clear, because at the same time the slip velocities are higher in the new model.

The potential of the new model is further illustrated in Figure 7. This shows the traction forces F_x and F_y for situation in which a modest amount of spin creepage is involved ($\phi = 0.55\,mrad/mm$, i.e. contact angle $\delta \approx 20°$). The data that are used are the same as described above, except that the contact patch is now elongated in rolling direction ($a = 8.9, b = 4.45\,mm$, aspect ratio $a/b = 2$). Further the results of Polach's method are included in the graph.

Figure 7 shows that altough the longitudinal force agrees well between Polach's method and the new approach, there are substantial differences in the lateral force. The interfacial layer in the new model appears to considerably reduce the effect of spin creepage. Of course the situation is more complex, changes for instance with the wheel load, curvatures, amount of spin and also when lateral creep is introduced. Still this demonstrates that there are significant differences between different theories. Therefore additional measurements should be performed in which spin creepage is involved, in order to better judge upon the merits of the different models that are now available.

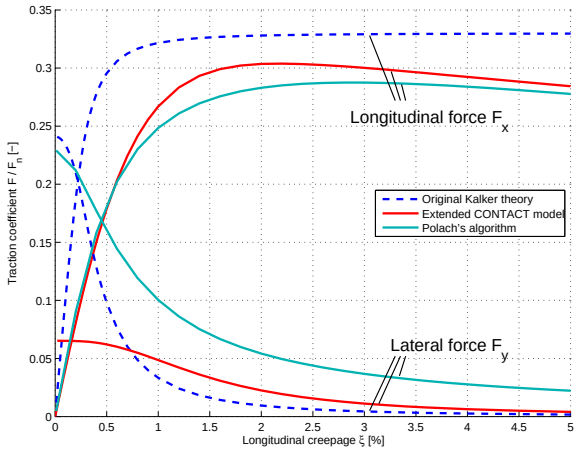

Figure 7: *Modeled longitudinal and lateral traction forces for steady running through a curve, with mild spin creepage.*

5 OTHER DEVELOPMENTS

5.1 Improvement of the calculation speed

A 100-fold speed-up of solving the normal contact problem is achieved by a fast computation of matrix-vector products using the Fast Fourier Transform (FFT). This relies on the special structure of the matrix that is employed in CONTACT, which arises because of the half-space approach and the use of rectangular discretisation elements. In contrast to earlier works where FFTs are used for computing contact problems, no simplifications or approximations are made. The exact same contact problem is solved as before, such that there is no effect whatsoever on the computational accuracy. Using the FFT the computational complexity is reduced from $\mathcal{O}(n^2)$ to $\mathcal{O}(n\log(n))$. This gives significant speed-up if n is large; a 100-fold speed-up is achieved for grid discretisations of $n = 100 \times 100$ points or more (Table 1).

The matrix $\mathbf{A}$ that occurs in CONTACT is a so-called "block-Toeplitz with Toeplitz blocks" (BTTB) matrix. (Toeplitz matrix: constant along each diagonal; block-Toeplitz: the same on the structure of matrix blocks.) Therefore the matrix-vector product is like the 2D convolution of surface tractions $\mathbf{p}$ with influence coefficients. The matrix is represented by a grid of size $2mx \cdot 2my$, twice larger than the potential contact area. The tractions are embedded in an array of the same size and padded with zeros. Then both arrays are transformed by 2D FFT's. The convolution in the spatial domain amounts to multiplication in the Fourier domain. This gives the Fourier transform of the displacements $\mathbf{u}$, which is back-transformed in $\mathcal{O}(n\log(n))$ time.

The performance data are shown in Table 1. These concern an investigation of the shape of the contact patch for a wheel with S1002 profile on a rail with UIC60 pro-

			N = 0: *pen* prescribed			N = 1: F_n prescribed		
resolution	grid	ncon	v11.1	v12.1	fac	v11.1	v12.1	fac
$\delta x = \delta y = 0.1\,mm$	70×80	3150	$4.3\,s$	$0.3\,s$	14	$12.8\,s$	$0.6\,s$	21
$\delta x = \delta y = 0.05\,mm$	140×160	12900	$81\,s$	$1.7\,s$	48	$245\,s$	$3.9\,s$	63
$\delta x = \delta y = 0.025\,mm$	280×320	50800	$1958\,s$	$17.3\,s$	113	$5104\,s$	$35.5\,s$	144

Table 1: *Calculation times for CONTACT versions 11.1 and 12.1 and corresponding speedup factors for solving a case with a "worn" S1002 wheel on UIC60 rail at* $6.2\,mm$ *lateral displacement.*

file. The wheelset is displaced over $6.2\,mm$ such that the contact is just moving from the tread to the flange. No yaw is incuded in this case. The resulting shape of the contact area is shown in Figure 8. The jagged edges are due to the way in which the profiles are prescribed in this case. Irregularities occur in the profiles for instance due to the way that interpolation is applied. Small irregularities in the profiles already have marked influence on the pressures and on where the actual contact occurs. The irregularities are retained here in order to put the solvers to the test, and to demonstrate the capabilities with respect to rough contacts too.

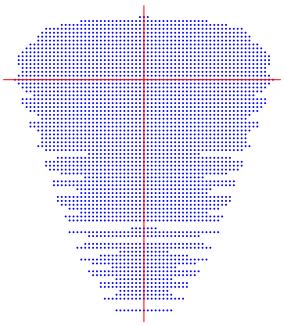

Figure 8: *Element division for* 70×80 *performance test.*

The computation of tangential contact problems has been accelerated too, but to a much lesser extent. A new variant of the Gauss-Seidel technique was found that works well on the steady-state rolling contact problem [14]. In 2D problems (line contact) the number of iterations and consequent computing time are reduced by an order of magnitude. In 3D contact problems the speed up is a factor 3, and the robustness is increased as well. Unfortunately, the FFT cannot yet be applied to the tangential problem. The reason for this is that its current solver does not contain matrix-vector products. Therefore we investigate new solver strategies that work and allow for the use of FFTs.

5.2 Interface to SIMPACK Rail

Over the years it was recognized that the CONTACT software was a "research code" and is difficult to use, requiring many steps of the user in order to get the problem specified and the results out of it. After the previous CM conference in Florence, 2009, the software was polished up a lot and we decided to make it publicly available [15]. The documentation of the input file was improved, and the program is much more forgiving now if errors are made. However, the file-based interface can still be qualified as "bare".

A new step along these lines is an interface that is created by which CONTACT is incorporated in SIMPACK Rail [18]. This allows for using CONTACT in vehicle system dynamics calculations with the SIMPACK software. All the preparations are then performed transparently and fully automatically: setting the relative positions of the wheel and rail, searching for the initial contact point, rotation of the wheel and rail profiles to a contact-local coordinate system, and calculation of the creepages. The main purpose of the interfacing is to deliver the distribution of surface tractions, which are input to wheel and rail damage mechanisms and to the calculation of wear. A further capability of the interface is to improve the simulation of the dynamic behavior of vehicles. As a side effect the pressures and shear tractions can be inspected visually as well. In that case SIMPACK is used as an extremely powerful pre-processor for generating the inputs to the CONTACT program.

6 SUMMARY AND OUTLOOK

In this paper we described recent and ongoing developments with respect to the CONTACT model for the wheel/rail contact forces. The results show a significant improvement in reproducing measured traction forces compared to Kalker's original theories. At the same time this changes the detailed results inside the contact patch, sometimes quite drastically. This makes us humble and aware of our still limited insight in the precise processes at the microscopic scales, and makes us call for additional measurements.

Our final goal is to compute the surface tractions and micro-slip velocities in the contact interface reliably in a wide range of circumstances. This requires primarily the proper understanding and implementation of the friction behavior, including the roles of fluids and temperature in the interface. Further extensions are called for with respect to conformal contact, plasticity effects and maybe roughness as well. We expect to be able to contribute to these areas in the coming years.

REFERENCES

[1] M. Acquati and E.E. Magel. Preliminary wheel/rail interface study: what benefits? In Bracciali [2].

[2] A. Bracciali, editor. *Proceedings of the 8th International Conference on Contact Mechanics and Wear of Rail/Wheel Systems*. Firenze, Italy, 2009.

[3] J.H. Dieterich. Modeling of rock friction 1. Experimental results and constitutive equations. *Journal of Geophysical Research*, 84:2161–2168, 1979.

[4] B. Engel, H.P. Beck, and J. Alders. Verschleißreduzierende Rad-schlupfregelung mit hoher Kraftschlussausnutzung. *Elektrische Bahnen*, 96:201–209, 1998.

[5] J.G. Giménez, A. Alonso, and E. Gómez. Introduction of a friction coefficient dependent on the slip in the FASTSIM algorithm. *Vehicle System Dynamics*, 43:233–244, 2005.

[6] K. Hou, J. Kalousek, and E. Magel. Rheological model of solid layer in rolling contact. *Wear*, 211:134–140, 1997.

[7] W. Kik and J. Piotrowski. A fast approximate method to calculate normal load at contact between wheel and rail and creep forces during rolling. In I. Zobory, editor, *Proceedings of the 2nd Mini Conference on Contact mechanics and Wear of Wheel/Rail systems*, Budapest, Hungary, 1996.

[8] E. Magel and Y. Liu. Study of friction - measurement, analysis and practical implications for the wheel/rail contact. In Bracciali [2], pages 239–245.

[9] J. Piotrowski. Kalker's algorithm Fastsim solves tangential contact problems with slip-dependent friction and friction anisotropy. *Vehicle System Dynamics*, 48(7):869–889, 2010. DOI: 10.1080/00423110903178495.

[10] O. Polach. Creep forces in simulations of traction vehicles running on adhesion limit. *Wear*, 258:992–1000, 2005.

[11] O. Polach, M. Berg, and S.D. Iwnicki. Chapter 12: Simulation. In S.D. Iwnicki, editor, *Handbook of Railway Vehicle Dynamics*, pages 359–421. CRC Press, Boca Raton, 2006.

[12] A. Ruina. Slip instability and state variable friction laws. *Journal of Geophysical Research*, 88:10359–10370, 1983.

[13] C. Tomberger, P. Dietmaier, W. Sextro, and K. Six. Friction in wheel-rail contact: a model comprising interfacial fluids, surface roughness and temperature. *Wear*, 271:2–12, 2011.

[14] E.A.H. Vollebregt. Improving the speed and accuracy of the frictional rolling contact model "CONTACT". In B.H.V. Topping, J.M. Adam, F.J. Pallarés, R. Bru, and M.L. Romero, editors, *Proceedings of the 10th International Conference on Computational Structures Technology*, Stirlingshire, United Kingdom, 2010. Civil-Comp Press.

[15] E.A.H. Vollebregt. User guide for CONTACT, Vollebregt & Kalker's rolling and sliding contact

model. Technical Report TR09-03, version 12.2, VORtech, 2012. See `www.kalkersoftware.org`.

[16] E.A.H. Vollebregt, S.D. Iwnicki, G. Xie, and P. Shackleton. Assessing the accuracy of different simplified frictional rolling contact algorithms. *Vehicle System Dynamics*, 50(1):1–17, 2012. DOI: 10.1080/00423114.2011.552618.

[17] E.A.H. Vollebregt and H.M. Schuttelaars. Quasi-static analysis of 2-dimensional rolling contact with slip-velocity dependent friction. *J. of Sound and Vibration*, 331(9):2141–2155, 2012. doi:10.1016/j.jsv.2012.01.011.

[18] E.A.H. Vollebregt, C. Weidemann, and A. Kienberger. Use of "CONTACT" in multi-body vehicle dynamics and profile wear simulation: Initial results. In S.D. Iwnicki et.al., editor, *Proceedings of the 22nd International Symposium on Dynamics of Vehicles on Roads and Tracks*, 2011.

[19] E.A.H. Vollebregt and P. Wilders. FASTSIM2: a second order accurate frictional rolling contact algorithm. *Comput.Mech.*, 47(1):105–116, 2010. DOI: 10.1007/s00466-010-0536-7.

[20] P. Wriggers. *Computational Contact Mechanics, 2nd ed.* Springer, Heidelberg, 2006.